Retrospective Application of Transposon-Directed Insertion Site Sequencing to a Library of Signature-Tagged Mini-Tn5Km2 Mutants of *Escherichia coli* O157:H7 Screened in Cattle[▽][†]

Sabine E. Eckert,[1][‡] Francis Dziva,[2][‡] Roy R. Chaudhuri,[3][‡] Gemma C. Langridge,[1][‡] Daniel J. Turner,[1][§]
Derek J. Pickard,[1] Duncan J. Maskell,[3] Nicholas R. Thomson,[1] and Mark P. Stevens[4]*

*The Wellcome Trust Sanger Institute, Wellcome Trust Genome Campus, Hinxton, Cambridge CB10 1SA, United Kingdom[1];
Enteric Bacterial Pathogens Laboratory, Institute for Animal Health, Compton, Berkshire RG20 7NN, United Kingdom[2];
Department of Veterinary Medicine, University of Cambridge, Madingley Road, Cambridge CB3 0ES,
United Kingdom[3]; and Roslin Institute and Royal (Dick) School of Veterinary Studies, University of
Edinburgh, Bush Farm Road, Roslin, Midlothian EH25 9RG, United Kingdom[4]*

Massively parallel sequencing of transposon-flanking regions assigned the genotype and fitness score to 91% of *Escherichia coli* O157:H7 mutants previously screened in cattle by signature-tagged mutagenesis (STM). The method obviates the limitations of STM and markedly extended the functional annotation of the prototype *E. coli* O157:H7 genome without further animal use.

Enterohemorrhagic *Escherichia coli* (EHEC) strains comprise a subset of Shiga toxin-producing *E. coli* strains that cause acute enteritis in humans (2). Infections may be complicated by severe sequelae and are frequently acquired via contact with ruminant feces. The molecular mechanisms underlying colonization of the ruminant intestines by EHEC are incompletely understood. Previously, we screened a library of 1,900 EHEC O157:H7 mutants for their ability to colonize bovine intestines by signature-tagged mutagenesis (STM) (6). STM relies on a panel of transposons harboring unique oligonucleotide tags. The tags can be detected by amplification and hybridization, enabling the composition of complex pools to be analyzed before and after inoculation of animals. Mutants that are negatively selected *in vivo* relative to the inoculum are inferred to lack a gene required for colonization or survival, which can be identified by isolation and sequencing of transposon-flanking regions (16).

Our analysis focused on the prototype *E. coli* O157:H7 strain EDL933, for which the chromosome and plasmid sequences are known (1, 18). Of the 1,900 signature-tagged mutants screened, 101 were underrepresented in pools recovered from feces 5 days postinoculation of calves (6). The transposon insertion site could be mapped in 79 such mutants, identifying 59 different genes influencing colonization (6). Thirteen attenuating mutations were mapped to the locus of enterocyte effacement (LEE), which encodes a type III secretion system

(T3SS) required for the formation of "attaching and effacing" lesions. The role of T3SS components in intestinal colonization was subsequently confirmed with defined mutants (6, 17) and by screening of 480 signature-tagged mutants of EHEC O26:H⁻ from calves (27). STM also detected attenuating mutations in genes encoding secreted substrates of the T3SS (*espD*, *map*, and *nleD*) (6).

Though STM has provided valuable insights into the genetic basis of virulence of microbes, it is limited by the number of unique tags and the effort required to construct libraries and map attenuating mutations. Moreover, only negatively selected mutants tend to be investigated and subjective judgments are required to compare signal intensities relative to the input and coscreened mutants. Functional annotation of the *E. coli* O157:H7 genome in reservoir hosts is further hindered by the cost of using large animals at a high level of disease containment. Recently, several protocols have been described that permit the simultaneous assignment of the genotype and fitness score for mutants screened in pools. Transposon-directed insertion-site sequencing (TraDIS) exploits Illumina sequencing to obtain the sequence flanking each transposon insertion (11). The massively parallel nature of such sequencing permits comparison of the number of specific reads derived from inocula and output pools recovered from animals, providing a numerical measure of the extent to which mutants were selected *in vivo*. TraDIS obviates the need to construct and array uniquely tagged mutants and to subclone and sequence attenuating mutations, yielding substantial time and cost savings. TraDIS-like methods have defined the essential gene complement of *Salmonella enterica* serovar Typhi (11) and *Streptococcus pneumoniae* (28) and have identified genes influencing *Haemophilus influenzae* pathogenesis (7) and survival of the gut symbiont *Bacteroides thetaiotaomicron* (8).

We retrospectively applied TraDIS to assign the genotype and fitness score of EDL933 mutants previously screened in calves. This required the massively parallel sequencing of transposon-flanking regions in the input and output pools of

---

* Corresponding author. Mailing address: Roslin Institute and Royal (Dick) School of Veterinary Studies, University of Edinburgh, Bush Farm Road, Roslin, Midlothian EH25 9RG, United Kingdom. Phone: 44 131 527 4200. Fax: 44 131 440 0434. E-mail: Mark.Stevens@roslin.ed.ac.uk.
§ Present address: Oxford Nanopore Technologies, 4 Robert Robinson Way, Magdalen Science Park, Oxford OX4 4GA, United Kingdom.
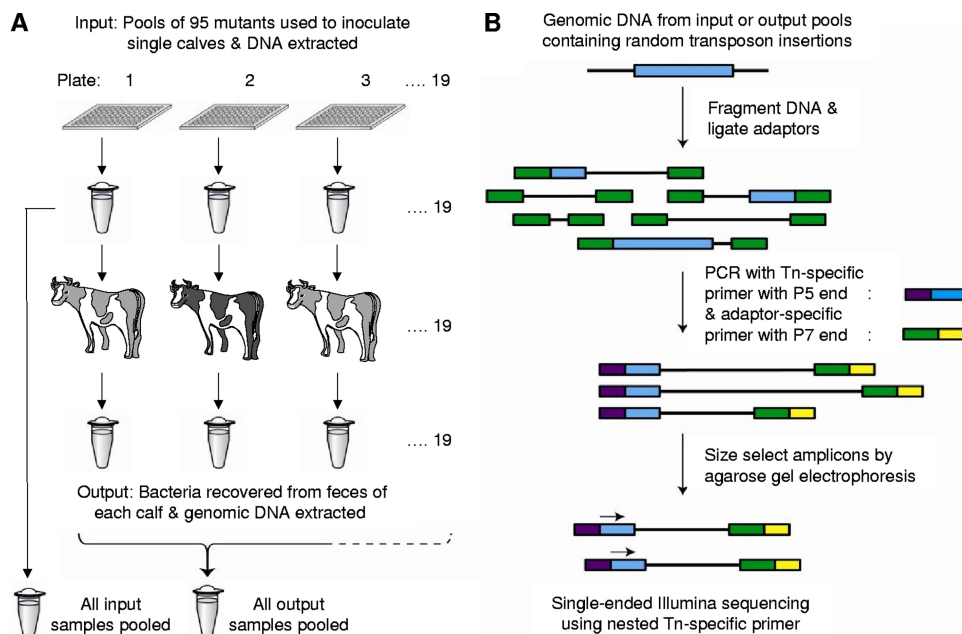‡ Contributed equally to the study.

FIG. 1. (A) Schematic representation of the screening of signature-tagged mutants of EDL933 from cattle. Uniquely tagged mini-Tn5Km2 mutants were arrayed in 96-well microtiter plates (1 well in each plate was left empty), and a total of 19 plates were separately screened by oral inoculation of a single calf (6). Genomic DNA was prepared from the pool of 95 mutants in the inoculum (input) and bacteria recovered from the feces of each infected calf (output). All 19 input samples and all 19 output samples were pooled for massively parallel sequencing of transposon-flanking regions, as schematically shown in panel B. Separately, genomic DNA from the input and output pools was fragmented, and Illumina paired-end adapters were ligated to the ends. This produces a mixture of fragments, some of which contain the transposon and the adjacent bacterial genome sequence. A 24-cycle PCR was performed with a transposon-specific primer and an adapter-specific primer, and products of the appropriate sizes were selected on an agarose gel. Amplicons were sequenced with a nested transposon-specific primer that anneals 10 nucleotides short of the end of the transposon.

EDL933 mini-Tn5Km2 mutants obtained by Dziva et al. (6), as schematically shown in Fig. 1. Adequate genomic DNA was retrieved for 19 of the mutant pools screened, comprising a total of 1,805 mutants. Genomic DNA from each input and output sample was quantified with a Nanodrop ND-1000 spectrophotometer (Thermo Fisher, Loughborough, United Kingdom). Equal amounts (1 µg) from all input and all output samples were pooled, and input and output pools were separately fragmented by ultrasonication with a Covaris adaptive focused acoustics instrument, to an average of 200 bp (19). Fragment libraries were prepared with the Illumina paired-end DNA sample preparation kit (PE-102-1001; Illumina, Little Chesterford, United Kingdom), according to the manufacturer's instructions, and quantified on an Agilent DNA1000 chip (Agilent, South Queensferry, United Kingdom). To form double-strand adapters, oligonucleotides Ind_Ad_T (5′-ACACTC TTTCCCTACACGACGCTCTTCCGATC*T-3′ [where the asterisk represents phosphorothioate) and Ind_Ad_B (5′-pG ATCGGAAGAGCGGTTCAGCAGGAATGCCGAGACCG ATCTC-3′) were annealed. The input and output DNA was ligated to the double-strand adapters and then quantified by quantitative PCR (qPCR) using the primers Ad_T_qPCR1 (5′-CTTTCCCTACACGACGCTCTTC-3′) and Ad_B_qPCR2 (5′-ATTCCTGCTGAACCGCTCTTC-3′) and SYBR green (Applied Biosystems, Warrington, United Kingdom). Two hundred nanograms of adaptor-ligated fragments was used to specifically amplify transposon insertion sites. Twenty-four cycles of PCR were performed with transposon-specific forward

primer MiniTn5-P5-3pr-3 (5′-AATGATACGGCGACCACC GAGATCTACACCTAGGCTGCGGCTGCACTTGTG-3′), which contains the Illumina P5 end for attachment to the flow cell, and reverse primer RInV3.3 (5′-CAAGCAGAAGACGG CATACGAGATCGGTACACTCTTTCCCTACACGACGC TCTTCCGATCT-3′, containing the Illumina P7 end). PCR products were size separated on an agarose gel, and fragments of 350 to 450 bp were excised and recovered with QiaExII gel extraction columns (Qiagen, Crawley, United Kingdom) following the manufacturer's instructions, but without heating (19). DNA was eluted in 30 µl of elution buffer, and quantified by qPCR with standards of known concentration, using primers Syb_FP5 (5′-ATGATACGGCGACCACCGAG-3′) and Syb_RP7 (5′-CAAGCAGAAGACGGCATACGAG-3′) (19).

The DNA fragment libraries were sequenced for 37 cycles according to the manufacturer's instructions on single end flow cells by an Illumina GAII sequencer, using the custom sequencing primer MiniTn5-3pr-seq3 (5′-TAGGCTGCGGCTG CACTTGTGTA-3′), which binds 10 bp from the transposon end. There were 12.6 and 13.3 million reads obtained for the input and output pools, respectively (European Nucleotide Archive accession no. ERP000368). Totals of 12.1 million (96.3%) of the input reads and 12.4 million (93.7%) of the output reads contained perfect matches to the 3′ end of mini-Tn5Km2 (3), and these reads were included in downstream analyses. Transposon-derived sequence was removed from each read with a custom Perl script available from the authors. The remainder of each sequence read was mapped to the

EDL933 chromosome and pO157 with NovoAlign (Novocraft Technologies Sdn Bhd, Selangor, Malaysia). Totals of 9.9 million input reads (78.4%) and 10.7 million output reads (80.6%) were mapped to unique positions in the EDL933 genome. Subsequent analyses were performed with R, version 2.8.0 (R Foundation for Statistical Computing, Vienna, Austria).

To quantify changes in the number of reads arising from specific insertions between the input and output, we adopted an approach suggested for RNA-Seq data analysis (15). The number of reads at each insertion location (x) was treated as a proportion of the total number of mapped reads (n), and a variance-stabilizing arcsine-root transformation was applied, converting each value of x to $\sqrt{n}$arcsin ($\sqrt{x/n}$). The transformed output values were divided by the equivalent input values to determine the fold change. To avoid infinite values derived from taking the log of 0, sequence counts of 0 were replaced with an arbitrary value of 0.5. $\log_2$ fold change values were calculated to represent the difference in abundance of each mutant in the output pools relative to the input and provide a measure of fitness. In our experience, TraDIS may overpredict the number of insertion sites due to a low-level background signal derived from incorrectly mapped or chimeric reads. To distinguish genuine inserts from this background signal, predicted insertion sites with fewer than 2^5 (i.e., 32) mapped reads were removed from the data set (see Fig. S1 in the supplemental material).

Of the 1,805 EDL933 mutants screened, TraDIS unambiguously assigned the insertion site and fitness score for 1,645, representing 855 different genes. Importantly, we assigned the genotype and fitness scores to 91.1% of the mutants analyzed, where previously we only identified the insertion site in 4.2% of mutants owing to the constraints of STM (6). Insertions were in general well distributed, although there are AT-rich regions where insertions are overrepresented (Fig. 2), as may be expected as mini-Tn5Km2 preferentially inserts at TA dinucleotides. Table S1 in the supplemental material lists the insertion site and $\log_2$ fold change relative to input for each mutation.

Figure S2 in the supplemental material shows a histogram of $\log_2$ fold change values obtained for all the mutants. This distribution was modeled by fitting a bimodal normal distribution using the R package mixdist (13) (Fig. S2). This model represents the mutants as a mixture of two distinct populations. Most of the mutants show no attenuation, with no clear change in abundance relative to the input pool and a normal distribution of $\log_2$ fold change values with a mean close to 0. Attenuated mutants show lower $\log_2$ fold change values, with a mean of approximately -3. The model suggests that a $\log_2$ fold change of -1 (equivalent to a 2-fold decrease in the abundance of the mutant in the output pool relative to the input) is a suitable cutoff value to identify most of the attenuated mutants while restricting the number of false positives to an acceptable level.

Seventy-two insertions were detected by both STM and TraDIS, 86.1% of which were negatively selected in both cases and 72.2% of which showed at least -1 $\log_2$ fold change or greater by TraDIS (see Table S1 in the supplemental material). Though STM screening of EDL933 mutants in calves identified 13 attenuating mutations in LEE genes (6) and was considered exhaustive at the time, TraDIS identified 54 insertions in the LEE in 21 different genes. By TraDIS, all LEE mutants were negatively selected, except those with insertions in *rorf1* or the region between *ler* and *espG* (Fig. 3). Insertions in the LEE-flanking regions were not attenuating. Mutations in predicted T3SS structural components were strongly negatively selected, with the exception of a single insertion in a gene of unknown function (*rorf8*). Several LEE genes were disrupted many times, producing comparable fitness scores. Variance in the scores for a given gene may reflect differences in competition dynamics in the pools in which the mutants were screened. TraDIS found 5 attenuating mutations in *eae*, encoding intimin and 3 mutations in *tir*, encoding the translocated intimin receptor. These were missed by STM, even though intimin and Tir play key roles in intestinal colonization of cattle by *E. coli* O157:H7 (22, 29). TraDIS also identified mutations in 29 of the 39 type III secreted effectors of *E. coli* O157:H7 verified by Tobe et al. (26) (see Table S2 in the supplemental material). Mutants with insertions in several LEE-encoded effectors (EspF, EspB, Tir, Map, EspH, and EspZ) were all negatively selected, consistent with the role of such effectors in intestinal persistence of *Citrobacter rodentium* in mice (4) and *E. coli* O157:H7 in rabbits (20). Of the non-LEE-encoded effectors, several appeared to play little or no role (e.g., NleG, NleH, EspY1, and EspY4) (Table S2), whereas mutations in the genes coding for the others were attenuating. Among the latter was *z1829*, encoding EspK, an effector missed by STM but which influences persistence of EHEC in calves (27, 30). Though several effector phenotypes have been independently verified, we caution that some attenuating mutations identified by STM could not be reproduced when mutants were tested in isolation (e.g., *map*) (6) or by coinfection with the parent strain (e.g., *nleD*) (14), possibly due to the distinct selection pressure exerted by combining 95 mutants during the library screen.

Analysis of signature-tagged mutants of EHEC O26:H$^-$ in calves indicated that the cytotoxins EspP and enterohemolysin may promote intestinal colonization (27). Though mutants with defects in these genes were not detected in the EDL933 STM screen (6), TraDIS revealed that several such mutants were represented in the library and were generally negatively selected in calves. Three of four EDL933 *espP* mutants were attenuated by TraDIS (see Table S1 in the supplemental material), consistent with the modest attenuation of a defined *espP* mutant in calves (5). Nine of 11 mutants with defects in the enterohemolysin (EHEC-*hly*) operon were negatively selected by TraDIS, supporting the attenuation of an *ehxA* mutant of EHEC O26:H$^-$ in calves (27). EhxA appears not to play a significant role in rectal colonization in steers (22); however, the latter study involved rectal application of the mutant to ruminant steers, without passage through the intestines. Eight insertions were detected in *l7031/tagA*, which encodes a zinc metalloprotease that cleaves C1-esterase inhibitor (StcE) (12), promotes adherence (9), and modulates neutrophil function (25). StcE mutants were generally underrepresented in calves, as were mutants with insertions in the EtpCD type II secretion system required for StcE secretion, consistent with the role of this system in colonization of rabbits (10). Seventeen mutations were detected in the gene encoding the large clostridial toxin homolog L7095/ToxB, though only 7 were negatively selected by greater than -1 $\log_2$ fold change.
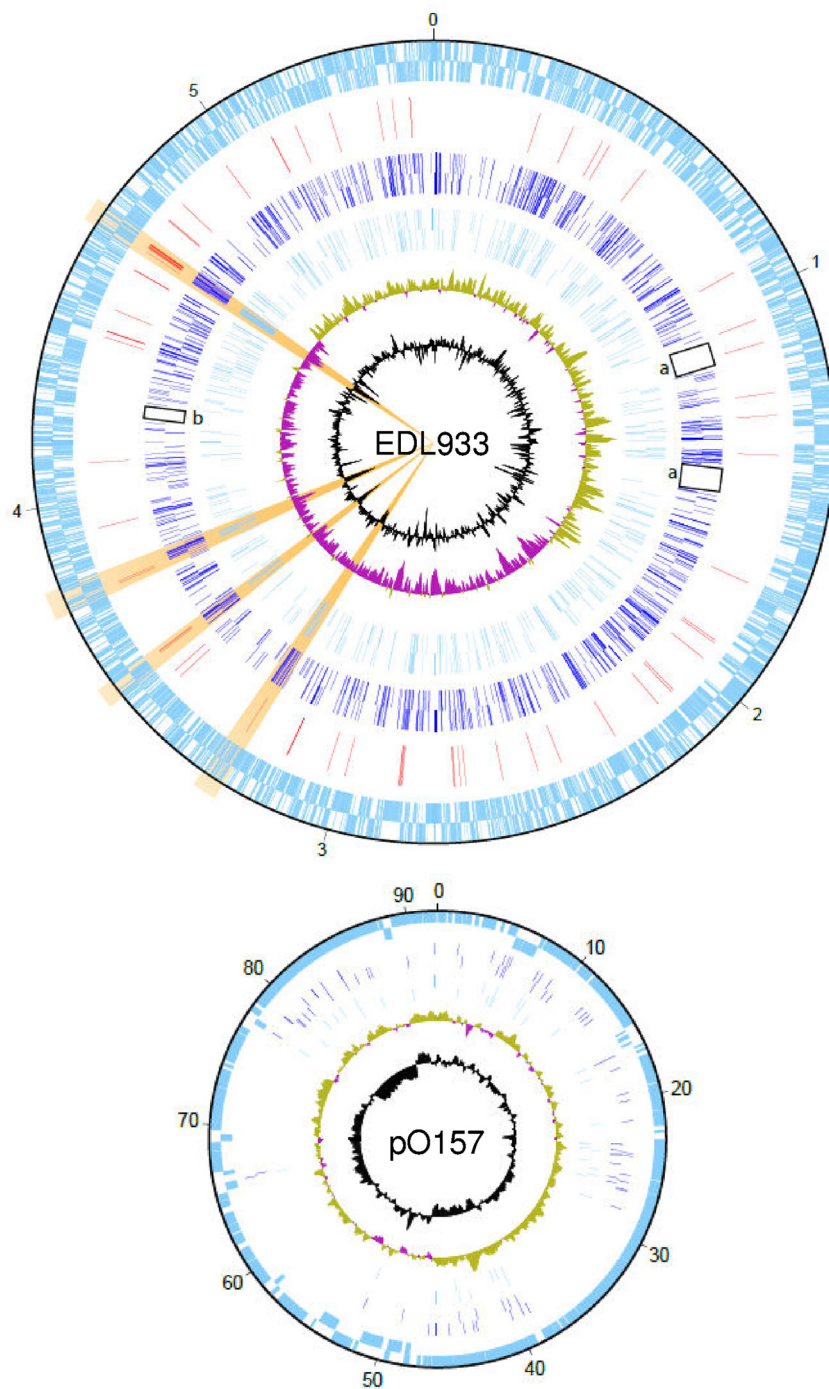
FIG. 2. Circular diagrams of the *E. coli* O157:H7 strain EDL933 chromosome and pO157 plasmid showing the locations of transposon insertions. For the chromosome, from the outside in, circle 1 indicates the positions of all the coding sequencer (CDS) transcribed in a clockwise and anticlockwise direction, respectively (light blue); circle 2 indicates the attenuating transposon insertions mapped by STM (6) (red); circle 3 indicates all transposon insertions mapped by TraDIS analysis of 1,805 of the same mutants screened by STM (dark blue); circle 4 indicates insertions mapped by TraDIS that were negatively selected by at least $-1 \log_2$ fold change (light blue); and circle 5 shows GC bias $[(G-C)/(G+C)]$. Khaki indicates values that are >1, and purple indicates values that are <1. Circle 6 shows the percentage of G+C content (black); regions with a high percentage of A+T content showing overrepresentation of insertions are highlighted in orange, including the LEE. a, duplicated O islands where transposon insertions cannot be mapped by TraDIS; b, region containing essential genes encoding ribosomal components, (e.g., *rps*, *rpl*, and *rpm*). Numbers indicate megabase pairs along the genome. For the plasmid, the outer circle represents all CDS; circle 2 represents all transposon insertions mapped by TraDIS, circle 3 represents insertions mapped by TraDIS that were negatively selected by at least $-1 \log_2$ fold change, circle 4 represents GC bias $[(G-C)/(G+C)]$. Khaki indicates values that are >1, and purple indicates values that are <1. Circle 5 represents the percentage of G+C content (black). Numbers indicate thousands of base pairs.
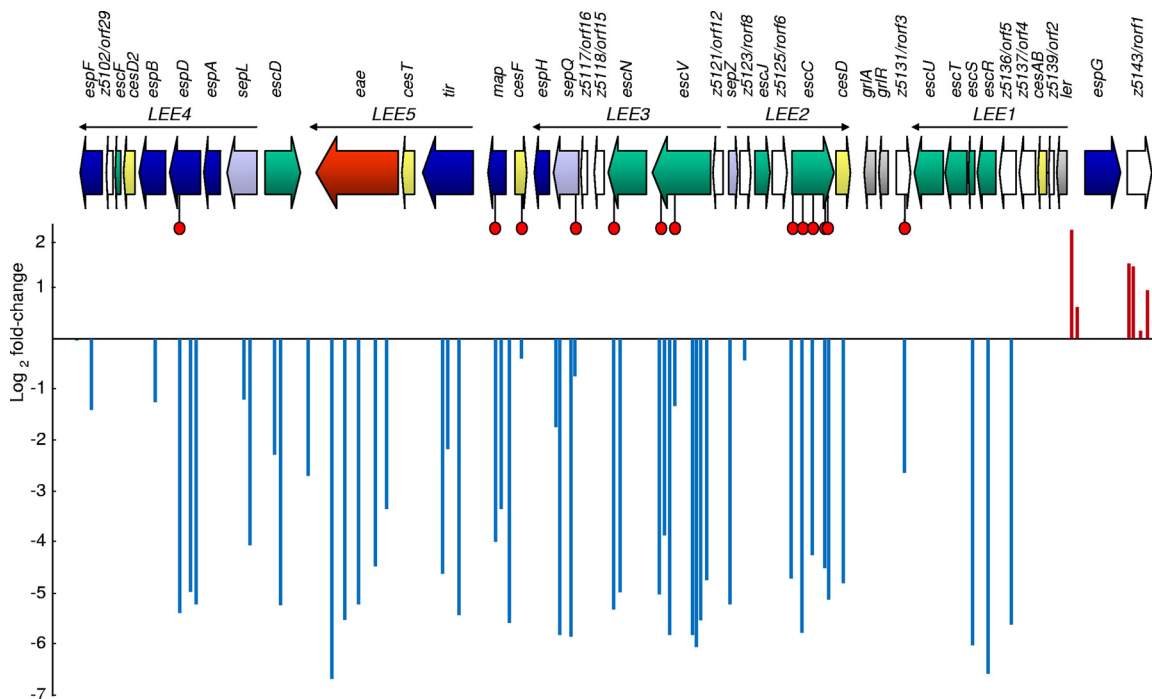
FIG. 3. Organization of the *E. coli* O157:H7 LEE showing the location of attenuating mutations mapped by STM (red pins) and the insertion site and fitness score of mutants identified by TraDIS (lower panel). Color key for box arrows: green, Esc (secretion apparatus); blue, Esp (secreted protein); yellow, Ces (chaperone); lilac, Sep proteins; red, intimin; gray, regulators; white, hypothetical open reading frame.

This relatively weak phenotype is consistent with the phenotype of a defined *E. coli* O157:H7 *toxB* mutant in calves (24). Other genes carried by pO157 that were missed by STM but putatively linked to colonization by TraDIS include *katP* (catalase-peroxidase), *l7029/msbB* (lipid A myristoyl transferase), and a gene of the linked *ecf* operon (*l7026*).

TraDIS faithfully reproduced the fitness defect of mutants detected by STM that are impaired in O-antigen biosynthesis (e.g., *manC*, *per*, *wbdP*, and *wzy*), consistent with the phenotype of an *E. coli* O157:H7 perosamine synthetase (*per*) mutant in steers (23). It also identified other attenuating mutations missed by STM that affect this process, as well as other pathways implicated in bacterial survival *in vivo*, such as aromatic amino acid biosynthesis (*aroA*) and iron storage (*ftn*). Of further interest, TraDIS identified an attenuating mutation in the catalytic subunit of Shiga toxin 1 (*stx1A*). Previously, STM identified an attenuating mutation downstream of the toxin genes in prophage CP-933V but upstream of those involved in bacterial lysis. The attenuation of the *stx1A* mutant supports the finding that Stx1 promotes intestinal colonization of mice by *E. coli* O157:H7 (21).

In common with other methods for screening pools of random mutants, TraDIS describes single gene-phenotype relationships and does not account for functional redundancy. Rarely, mutants may also contain more than one transposon insertion, harbor a secondary mutation of another kind, or possess polar insertions affecting the expression of nearby genes. These limitations impose a formal requirement to confirm mutant phenotypes via the evaluation of nonpolar mutant and repaired or *trans*-complemented strains. The number of mutants that can be simultaneously screened will also be con-

strained by the requirement to obtain an output pool of an adequate size at a time postinoculation sufficient for attenuation to be evident. It is estimated that if 100 mutants are screened, the output pool must comprise at least 10,000 colonies in order to state at the 95% confidence interval that specific mutants are absent due to attenuation as opposed to chance (6). Moreover, at high pool complexities, stochastic loss of mutants may occur if the number of mutants exceeds a "bottleneck" above which individual mutants in the population no longer have an equal chance of establishing themselves in the host. Such limitations are balanced by the ability of massively parallel sequencing of mutant libraries to derive vastly richer functional annotation of pathogen genomes than can be obtained by earlier methods.

In conclusion, TraDIS validated and substantially extended our analysis of signature-tagged *E. coli* O157:H7 mutants in cattle. It described the genotype and fitness score for 91.1% of mutants screened, unlocking hundreds of novel phenotypes with no further animal use. It represents a significant advance toward the principles of reduction, refinement, and replacement of animals in research and is relatively inexpensive to apply *de novo* or retrospectively. The procedures described herein relate to transposons that have been extensively used in other microbes (reviewed in reference 16) and can therefore be widely applied to derive quantitative data for functional annotation of microbial genomes.

REFERENCES

1. **Burland, V., et al.** 1998. The complete DNA sequence and analysis of the large virulence plasmid of *Escherichia coli* O157:H7. Nucleic Acids Res. **26:**4196–4204.
2. **Croxen, M. A., and B. B. Finlay.** 2010. Molecular mechanisms of *Escherichia coli* pathogenicity. Nat. Rev. Microbiol. **8:**26–38.
3. **de Lorenzo, V., M. Herrero, U. Jakubzik, and K. N. Timmis.** 1990. Mini-Tn5 transposon derivatives for insertion mutagenesis, promoter probing, and chromosomal insertion of cloned DNA in Gram-negative eubacteria. J. Bacteriol. **172:**6568–6572.
4. **Deng, W., et al.** 2004. Dissecting virulence: systematic and functional analyses of a pathogenicity island. Proc. Natl. Acad. Sci. U. S. A. **101:**3597–3602.
5. **Dziva, F., et al.** 2007. EspP, a type V-secreted serine protease of enterohaemorrhagic *Escherichia coli* O157:H7, influences intestinal colonization of calves and adherence to bovine primary intestinal epithelial cells. FEMS Microbiol. Lett. **271:**258–264.
6. **Dziva, F., P. M. van Diemen, M. P. Stevens, A. J. Smith, and T. S. Wallis.** 2004. Identification of *Escherichia coli* O157:H7 genes required for colonisation of the bovine gastrointestinal tract using signature-tagged mutagenesis. Microbiology **150:**3631–3645.
7. **Gawronski, J. D., S. M. S. Wong, G. Giannoukos, D. V. Ward, and B. J. Akerley.** 2009. Tracking insertion mutants within libraries by deep sequencing and a genome-wide screen for *Haemophilus* genes required in the lung. Proc. Natl. Acad. Sci. U. S. A. **106:**16422–16427.
8. **Goodman, A. L., et al.** 2009. Identifying genetic determinants needed to establish a human gut symbiont in its habitat. Cell Host Microbe **6:**279–289.
9. **Grys, T. E., M. B. Siegel, W. W. Lathem, and R. A. Welch.** 2005. The StcE protease contributes to intimate adherence of enterohemorrhagic *Escherichia coli* O157:H7 to host cells. Infect. Immun. **73:**1295–1303.
10. **Ho, T. D., B. M. Davis, J. M. Ritchie, and M. K. Waldor.** 2008. Type 2 secretion promotes enterohemorrhagic *Escherichia coli* adherence and intestinal colonization. Infect. Immun. **76:**1858–1865.
11. **Langridge, G. C., et al.** 2009. Simultaneous assay of every *Salmonella* Typhi gene using one million transposon mutants. Genome Res. **19:**2308–2316.
12. **Lathem, W. W., et al.** 2002. StcE, a metalloprotease secreted by *Escherichia coli* O157:H7, specifically cleaves C1 esterase inhibitor. Mol. Microbiol. **45:**277–288.
13. **Macdonald, P., and J. Du.** 2008. mixdist: finite mixture distribution models. R package, version 0.5-2. http://www.math.mcmaster.ca/peter/mix/mix.html.
14. **Marchés, O., et al.** 2005. Characterization of two non-LEE encoded type III secreted effectors, NleC and NleD, in attaching and effacing pathogens. Infect. Immun. **73:**8411–8417.
15. **Marioni, J. C., C. E. Mason, S. M. Mane, M. Stephens, and Y. Gilad.** 2008. RNA-seq: an assessment of technical reproducibility and comparison with gene expression arrays. Genome Res. **18:**1509–1517.
16. **Mazurkiewicz, P., C. M. Tang, C. Boone, and D. W. Holden.** 2006. Signature-tagged mutagenesis: barcoding mutants for genome-wide screens. Nat. Rev. Genet. **7:**929–939.
17. **Naylor, S. W., et al.** 2005. *Escherichia coli* O157:H7 forms attaching and effacing lesions at the terminal rectum of cattle and colonization requires the LEE4 operon. Microbiology **151:**2773–2781.
18. **Perna, N. T., et al.** 2001. Genome sequence of enterohaemorrhagic *Escherichia coli* O157:H7. Nature **409:**529–533.
19. **Quail, M. A., H. Swerdlow, and D. J. Turner.** 2009. Improved protocols for the Illumina genome analyzer sequencing system. Curr. Protoc. Hum. Genet. **62:**18.2.1–18.2.27.
20. **Ritchie, J. M., and M. K. Waldor.** 2005. The locus of enterocyte effacement-encoded effector proteins all promote enterohemorrhagic *Escherichia coli* pathogenicity in infant rabbits. Infect. Immun. **73:**1466–1474.
21. **Robinson, C. M., J. F. Sinclair, M. J. Smith, and A. D. O'Brien.** 2006. Shiga toxin of enterohemorrhagic *Escherichia coli* type O157:H7 promotes intestinal colonization. Proc. Natl. Acad. Sci. U. S. A. **103:**9667–9672.
22. **Sheng, H., J. Y. Lim, H. J. Knecht, J. Li, and C. J. Hovde.** 2006. Role of *Escherichia coli* O157:H7 virulence factors in colonization at the bovine terminal rectal mucosa. Infect. Immun. **74:**4685–4693.
23. **Sheng, H., J. Y. Lim, M. K. Watkins, S. A. Minnich, and C. J. Hovde.** 2008. Characterization of an *Escherichia coli* O157:H7 O-antigen deletion mutant and effect of the deletion on bacterial persistence in the mouse intestine and colonization at the bovine terminal rectal mucosa. Appl. Environ. Microbiol. **74:**5015–5022.
24. **Stevens, M. P., et al.** 2004. Mutation of *toxB* and a truncated version of the *efa-1* gene in *Escherichia coli* O157:H7 influences the expression and secretion of locus of enterocyte effacement-encoded proteins but not intestinal colonization in calves or sheep. Infect. Immun. **72:**5402–5411.
25. **Szabady, R. L., M. A. Lokuta, K. B. Walters, A. Huttenlocher, and R. A. Welch.** 2009. Modulation of neutrophil function by a secreted mucinase of *Escherichia coli* O157:H7. PLoS Pathog. **5:**e1000320.
26. **Tobe, T., et al.** 2006. An extensive repertoire of type III secretion effectors in *Escherichia coli* O157 and the role of lambdoid phages in their dissemination. Proc. Natl. Acad. Sci. U. S. A. **103:**14941–14946.
27. **van Diemen, P. M., F. Dziva, M. P. Stevens, and T. S. Wallis.** 2005. Identification of enterohemorrhagic *Escherichia coli* O26:H⁻ genes required for intestinal colonization in calves. Infect. Immun. **73:**1735–1743.
28. **van Opijnen, T., K. L. Bodi, and A. Camilli.** 2009. Tn-seq: high-throughput parallel sequencing for fitness and genetic interaction studies in microorganisms. Nat. Methods **6:**767–772.
29. **Vlisidou, I., et al.** 2006. Role of intimin-Tir interactions and the Tir-cytoskeleton coupling protein (TccP) in the colonization of calves and lambs by *Escherichia coli* O157:H7. Infect. Immun. **74:**758–764.
30. **Vlisidou, I., et al.** 2006. Identification and characterization of EspK, a type III secreted effector protein of enterohaemorrhagic *Escherichia coli* O157:H7. FEMS Microbiol. Lett. **263:**32–40.